

Conformational Flexibility is a Determinant of Permeability for Cyclosporin

Conan K. Wang*, Joakim E. Swedberg, Peta J. Harvey, Quentin Kaas, David J. Craik^{1,*}

¹Institute for Molecular Bioscience, The University of Queensland, Brisbane, Queensland, 4072, Australia

*Corresponding Authors:

Dr Conan Wang or Professor David J. Craik

Institute for Molecular Bioscience,

The University of Queensland,

Brisbane, QLD, 4072, Australia

Tel: +61-7-3346 2019

Fax: +61-7-3346 2101

E-mail: d.craik@imb.uq.edu.au

Abstract

Several cyclic peptides have been reported to have unexpectedly high membrane permeability. Of these, cyclosporin A is perhaps the most well-known example, particularly in light of its relatively high molecular weight. Observations that cyclosporin A changes conformation depending on its solvent environment led to the hypothesis that conformational dynamics is a prerequisite for its permeability; however, this hypothesis has been difficult to validate experimentally. Here, we use molecular dynamics simulations to explicitly determine the conformational behavior of cyclosporin A and other related cyclic peptides as they spontaneously transition between different environments, including through a lipid bilayer. These simulations are referenced against simulations in explicit water, chloroform, and cyclohexane and further validated against NMR experiments, measuring conformational exchange, nuclear spin relaxation, and 3D structures in membrane-mimicking environments, such as in DPC micelles, to build a comprehensive understanding of the role of dynamics. We find that conformational flexibility is a key determinant of the membrane permeability of cyclosporin A and similar membrane-permeable cyclic peptides, as conformationally constrained variants have limited movement into, then through and finally out of the membrane *in silico*. We envisage that a better understanding of dynamics might thus provide new opportunities to modulate peptide function and enhance their delivery.

Introduction

Peptides are promising alternatives to small molecules as drug modalities, and are particularly attractive because of their potential applications in the ‘undruggable’ target space of intracellular protein:protein interactions,¹ with several examples now available of peptides with promising activity profiles.²⁻⁵ However, a major challenge for peptides is their poor oral bioavailability, which limits their translation into drugs.

Cyclosporin A stands in the face of this criticism: it is one of the largest known cyclic peptides to have pharmaceutically tractable oral bioavailability since the initial pharmacokinetic studies in which it was characterized 50 years ago.⁶ This 11-residue peptide (Figure 1) was originally isolated from the fungus *Tolypocladium inflatum*^{7,8} and is currently used as an immunosuppressant, modulating the expression of inflammatory cytokines by binding to the cytosolic protein, cyclophilin.⁹ After oral administration, cyclosporin A must cross the enterocyte layer of the gastrointestinal tract, enter the systematic circulation and subsequently make its way into the lymphocytes. As a peptide, the voyage from gut to cytosol faces several challenges, requiring passage across multiple cellular membranes. Cyclosporin A is thought to rely on passive diffusion to accomplish this feat.^{10,11}

Studies on peptide permeability^{12,13} suggest that the cyclic backbone and N-methyl moieties of cyclosporin A are partly responsible for its ability to diffuse across membranes. These structural characteristics lead to the burial of polar groups, presumably resulting in favorable desolvation energies for the transition from an aqueous to a membrane phase. These findings for cyclosporin have furthermore been more generally exploited to enhance the membrane permeability of other small cyclic peptides.¹⁴⁻¹⁶ Other recent studies have expanded the knowledgebase of membrane-permeable cyclic peptides¹¹ as well as our understanding of the determinants of peptide permeability, raising awareness of the importance of lipophilicity, structure, solubility, and size, as well as the interplay between these factors.¹⁷⁻²²

Conformational polymorphism is another feature of cyclosporin A thought to be important for its membrane permeability.^{11,23,24} This hypothesis is based on structural analyses of cyclosporin A

that showed a dependence of its structure and dynamics on the solution environment,^{10,25-29} as highlighted in Figure 1. In chloroform, cyclosporin A predominantly adopts a single conformation characterized by an elongated shape with internal hydrogen bonds that hide the constituent donor and acceptor groups from the solvent.^{25,26} Hereafter, we refer to this conformation as the “closed” state. Although cyclosporin A is thought to adopt multiple conformations in water,¹⁰ experimentally determined structures in water are not available. Alternative structures to that formed in chloroform have been elucidated but these are of cyclosporin A bound to a protein target, typically cyclophilin.³⁰⁻³² Nevertheless, these structures provide the most reasonable representation of a non-chloroform, and potentially aqueous, state; we refer to these as the “open” conformations because of the increased exposure of the polar groups.

The hypothesis that conformational change (and so dynamics) of cyclosporin A facilitates its diffusion across membranes is easy to conceptualize but difficult to test experimentally because chemical modification to preference a particular conformation or tune structural rigidity would invariably change peptide lipophilicity and size, making it difficult to delineate the contribution of conformational flexibility. Predicted structures of cyclic peptides in implicit solvents of low and high dielectric constants that approximate aqueous and lipid environments, respectively, have been shown to be predictive of the propensity for membrane insertion.^{23,24} Instead of focusing on defined time-points during the permeation process, molecular dynamics offers a way to explicitly track conformational motion, resolving spatial and temporal dimensions as the peptide permeates through the membrane and in response to variations in simulation parameters, such as temperature.^{33,34} Several studies have examined the behavior of cyclosporin A in water and chloroform *in silico*.³⁵⁻³⁸ Early attempts were limited by their short simulation times (in the ps range),³⁵⁻³⁷ but more recent studies have shown the potential of extended simulations in these solvents to capture the landscape of conformations and inter-conversion rates between conformations, which can be used to rationalize differences in permeability.^{38,39} Here we extend these studies to new ground to look explicitly at the transition between different environments, such as aqueous and lipid phases.

In the current study our aim was to understand the contribution of dynamics to the membrane permeability of cyclic peptides. To build towards that goal, we first simulated cyclosporin A in simple solvents to validate the simulation parameters against NMR-derived data, and then moved to more complex systems that more accurately mimic cellular membranes, demonstrating the role of conformational flexibility in membrane permeability. Finally, we broadened the study to examine other membrane-permeable cyclic peptides. A better understanding of the membrane permeability of cyclic peptides might facilitate the future design of membrane-permeable and orally bioavailable peptides.

Methods

Chemicals and peptides

Deuterated acetonitrile (acetonitrile-d₃, 99.8%), chloroform (chloroform-d, 99.8%, with 0.03% v/v tetramethylsilane), cyclohexane (cyclohexane-d₁₂, 99.5%), and dodecylphosphocholine (dodecylphosphocholine-d₃₈, 98%) were purchased from Novachem. Cyclosporin A (≥98.5%) was purchased from Sigma Aldrich. Cyclosporin H (≥95%) was purchased from Cayman Chemicals.

NMR spectroscopy

NMR samples were prepared by dissolving dried peptide (1 mg) in 550 μL of the desired solvent mixture; i.e., 38–100% (v/v) acetonitrile-d₃ (mixed with water), pure chloroform-d, pure cyclohexane-d₁₂, or a mixture of dodecylphosphocholine-d₃₈ with water. Typically, samples were centrifuged at 13,000 rpm for 10 min to remove precipitate (which was observed for the cyclohexane sample) before data acquisition. One- and two-dimensional NMR spectra (¹H, ¹H TOCSY, NOESY) were recorded on a Bruker Avance 500 MHz spectrometer at the indicated temperatures. Mixing times of 80 and 200 ms were used for TOCSY and NOESY experiments, respectively. Spectra were processed with TopSpin (Bruker), phased and calibrated, and then assigned with CCPNMR software v2.4.2.⁴⁰ Chemical shifts in the ¹H dimension were referenced to internal 4,4-dimethyl-4-silapentane-1-sulfate or tetramethylsilane.

Relaxation measurements were carried out using Bruker Avance 500, 600, and 900 MHz spectrometers, as previously described.⁴¹ T₁ (spin-lattice) ¹³C relaxation times were measured using the Bruker pulse program hsqct1etgpsi3d.2. NMR spectra were acquired with a spectral width of 14 ppm over 2048 complex points in the ¹H dimension, and 12 ppm over 40 complex points in the ¹³C dimension. To determine T₁ values, 12 relaxation delays in the range of 0.01 to 2.5 s were used. A recycle delay of 2 s was used. Peak heights were measured in CCPNMR and fitted using a two-parameter fit exponential equation to determine T₁ values. Experiments were carried out in triplicate, with a different order of relaxation delays used in each experiment; the mean and standard deviation for the T₁ values were derived.

^{13}C NOEs were determined from the ratio of peak intensities from 2D ^1H - ^{13}C correlation spectra measured via double inept transfer using sensitivity improvement with decoupling during acquisition, using Bruker pulse program hsqcnoegpsi.2. A recycle delays of 2 s was used. NOE on and NOE off spectra were processed with a zero scaling factor, phased identically, and the intensities of the respective peaks were measured using CCPNMR software. Errors were calculated as the standard deviation over triplicate measurements.

The relaxation data were fitted to equations described in the model-free formalism using the ‘Solver’ function in Microsoft Excel, as previously described.⁴¹ Errors were estimated by fitting to simulated data generated using a Monte Carlo algorithm. The fits of the NOE values were given a 50% weighting compared to the T_1 values, to take into account the higher uncertainty in the experimental NOE measurements.⁴¹

Molecular dynamics

The solid-state structure of cyclosporin A crystallized from chloroform was used as the “closed” form (CCDC code: DEKSAN), whereas the solution-state structure bound to cyclophilin was used as the “open” form (PDB ID: 1CYA). The open form was selected by downloading, aligning, and visually inspecting structures of cyclosporin A (and its analogues) deposited in PDB (35 in total; i.e., 1BCK, 1C5F, 1CSA, 1CWA, 1CWB, 1CWC, 1CWF, 1CWH, 1CWI, 1CWJ, 1CWK, 1CWL, 1CWM, 1CWO, 1CYA, 1CYB, 1CYN, 1IKF, 1M63, 1MIK, 1QNG, 1QNH, 1XQ7, 2ESL, 2OJU, 2POY, 2RMA, 2RMB, 2RMC, 2WFJ, 2X7K, 2Z6W, 3BO7, 3CYS, 3EOV). The solid-state structure of cyclosporin H crystallized from methanol⁴² was used as the starting conformation in simulations. The solution structure of cyclic peptide 13 was used in our simulations;¹⁶ the structure of cyclic peptide 1 was derived from cyclic peptide 13 by removing the N-methyl groups *in silico*.

Force field parameters for the peptides were derived from the CHARMM27 force field. For non-standard amino acids, parameters for their side-chains were obtained from SwissParam (<http://www.swissparam.ch/>); parameters for their backbone regions were initially derived from the CHARMM27 force field, and later modified as described. Force field parameters for

chloroform were based on the rigid model of Dietz and Heinzinger⁴³ (which was previously shown to reproduce experimental liquid properties⁴⁴), parameters for cyclohexane were obtained from a CHARMM force field for ethers, and parameters for POPC were extracted from the CHARMM36 force field (which has been optimized for lipids).

Simulation protocols were modified from previously described methods for cyclic peptides in explicit solvent.^{41,45} Specifically, for simulations in a single solvent (i.e., chloroform, water, or cyclohexane only), a cubic box of solvent ($50 \times 50 \times 50 \text{ \AA}$) was constructed and the peptide was placed at the center. For simulations using a biphasic system (i.e., chloroform and water), a box ($80 \times 80 \times 100 \text{ \AA}$) filled with chloroform in the lower half and water in the upper half was constructed, and the peptide was placed at the center of the water partition. With harmonic restraints of $5 \text{ kcal}/(\text{mol \AA})$ on the centroid of the $C\alpha$ atoms and dihedral angles of cyclosporin A, each system was first minimized with 10,000 steps of conjugate gradient energy minimization using NAMD v2.11. This was followed by a 100-ps simulation in the canonical (NVT) ensemble and then 100 ps isothermal-isobaric ensemble (NPT) simulation at the experimental temperature and pressure, both with the harmonic restraints. A further equilibration of 1 ns was conducted before initiating production runs. The harmonic restraints on the dihedral angles were maintained for simulations of the constrained closed and open conformations, or were removed otherwise. Molecular dynamics simulations were performed using periodic boundary conditions. The particle mesh Ewald method with a real space cutoff of 12 \AA was used to treat Coulomb interactions and a force-switching function was applied to smooth Lennard-Jones interactions over the range of $10\text{--}12 \text{ \AA}$. All covalent hydrogen bonds were constrained by the SHAKE algorithm (or the SETTLE algorithm for water), permitting an integration time step of 2 fs. Coordinates were saved every 100 ps.

For simulations in a lipid/water system, a box ($80 \times 80 \times 100 \text{ \AA}$) was constructed, comprised of a POPC (1-palmitoyl-2oleoyl-*sn*-glycero-3-phosphocholine) lipid bilayer and the peptide placed in the aqueous phase. With harmonic restraints of $2 \text{ kcal}/(\text{mol \AA})$ on all non-hydrogen atoms and $5 \text{ kcal}/(\text{mol \AA})$ on all peptide dihedral angles, the system was first subjected to 10,000 steps of conjugate gradient minimization, followed by 490-ps NPT simulation. A Langevin thermostat

with a damping coefficient of 1 ps^{-1} was used to maintain the system temperature. The system pressure was maintained at 1 atm using a Langevin piston barostat. Initially, covalent hydrogen bonds were not constrained and an integration time step of 1 fs was used. Then, a 1.5-ns simulation was carried out with harmonic restraints of $2 \text{ kcal}/(\text{mol } \text{Å})$ on all heavy atoms, while maintaining harmonic restraints on peptide dihedral angles. Afterwards, all covalent hydrogen bonds were constrained by the SHAKE algorithm (or the SETTLE algorithm for water) and the integration time step was increased to 2 fs for a 4-ns simulation, while restraining all heavy atoms and peptide dihedral angles. Then, a 9-ns simulation with harmonic restraints of $2 \text{ kcal}/(\text{mol } \text{Å})$ on all peptide carbon atoms and $5 \text{ kcal}/(\text{mol } \text{Å})$ on all peptide dihedral angles and $2 \text{ kcal}/(\text{mol } \text{Å})$ on C1 carbon of all POPC lipids was carried out. Subsequently, restraints on the carbon atoms were removed for simulations of the constrained, closed and open conformations, and the system was equilibrated for a further 3 ns before carrying out production runs. Otherwise, all restraints were subsequently removed, and the system was equilibrated for 3 ns before production runs were conducted using ACEMD v1.6.0. Compared to simulations using NAMD v2.11, the cutoff was changed to 9 Å , and the integration time step was increased to 4 fs with the use of hydrogen mass re-partitioning as implemented in ACEMD.

Order parameters were calculated from the simulations by overlaying all snapshots from the trajectories to the structure of the first snapshot, as previously described.^{41,46} The approach has its limitations (e.g., it is sensitive to the quality of the structural alignments), but is useful for providing broad indications on the flexibility of the system being studied. For each snapshot, the unit vector along the $C\alpha$ - $H\alpha$ vector was obtained from its Cartesian co-ordinates and used in the following equation:

$$S^2 = \frac{3}{2} [\langle x^2 \rangle^2 + \langle y^2 \rangle^2 + \langle z^2 \rangle^2 + 2\langle xy \rangle^2 + 2\langle yz \rangle^2 + 2\langle xz \rangle^2] - \frac{1}{2}$$

, where $\langle \rangle$ denotes the average over all snapshots from the trajectory.

Results

Dynamics of cyclosporin A

We confirmed that the conformation is dependent on solution environment in a series of NMR studies of cyclosporin A in a range of solvent mixtures (Figure 2a). Cyclosporin A is sparingly soluble in water and thus we used deuterated acetonitrile/water mixtures in a first set of experiments to confirm the role of the solvent. In a predominantly aqueous environment (<40% CD₃CN content), the large number of peaks in the ¹H 1D NMR spectrum indicates the presence of at least three conformations in slow exchange on the μs-ms timescale. In general, increasing the acetonitrile concentration increases structural homogeneity as judged by a reduced number of spectral peaks. Indeed, the spectrum of cyclosporin A in pure acetonitrile indicates convergence to one major conformation (population >90%), consistent with previous findings.²⁸

The conformational homogeneity is even greater in pure chloroform, where the spectrum is dominated by just four peaks in the amide region of the spectrum—corresponding to the four backbone amides of cyclosporin A, and indicating one major conformation is present. This conformation is well characterized and is shown in Figure 1. A minor conformation (population <6%) has been reported and differs from the major conformation by *cis/trans* isomerization about an N-methylated peptide bond.²⁶ Overall the data suggest minimal conformational dynamics on the ms timescale (as assessed by NMR peak analysis) in chloroform. But what about faster motions not detected based on peak multiplicity?

We used NMR relaxation measurements to gain a more precise understanding of the backbone dynamics on the ns-timescale of cyclosporin A in chloroform (Figure 2b). ¹³C NMR spin-lattice (T₁) relaxation times and heteronuclear NOEs (hNOEs) for the C_α-H_α bonds were recorded at three field strengths (i.e., 500, 600, and 900 MHz) and interpreted according to the model-free formalism,⁴⁷ which provides values for the correlation time (reflecting the rate of rotational diffusion) and the order parameters (reflecting the amplitudes of local motions). For cyclosporin A in chloroform the overall correlation time was found to be 0.28 ns, with order parameters (S²) for individual backbone C_α sites ranging from 0.72 to 0.83 (mean of 0.78). This result is consistent with a partial analysis of backbone C_α dynamics reported earlier,⁴⁸ apart from two

outliers in that analysis that gave very low order parameters. The important conclusion to arise from this analysis is that individual backbone sites of cyclosporin A do have limited amplitude fast (sub ns-timescale) motions and this peptide is more flexible than other cyclic peptides with highly cross-braced structures, which typically exhibit S^2 values >0.8 .^{41,49} In other words, in any given conformation cyclosporin A is not completely rigid (S^2 values ~ 1.0 would be expected for a rigid molecule). These experimental solution state data provide a benchmark upon which to calibrate *in silico* simulations, as detailed below.

Simulations of the closed structure of cyclosporin A in chloroform

Since it is well established that the closed form of cyclosporin A is the main conformation in chloroform we explored whether this structure can be faithfully predicted *in silico*. Accordingly, a model of the closed form was placed in a box of explicit chloroform and subjected to molecular dynamics simulations. Over the course of the simulation runs at both 298 and 315 K, very little deviation from the starting structure was observed (Figure 3a). Increasing the temperature to 490 K resulted in increased local flexibility, as well as sporadic and significant deviations from the closed structure; however, the closed form was still the most frequently observed over the simulated time (Figures 3a and 3b).

We compared the order parameters calculated from the simulations to experimentally determined values and found that elevated temperature simulations better recreated the experimentally observed dynamics than the room temperature simulations (Figure 3c). Order parameters were calculated from the simulations by integrating the time-dependent fluctuations of the $C\alpha$ - $H\alpha$ bond vectors using a previously described approach.⁴⁶ Despite its limitations, the approach is suitable here because the simulation times are long relative to the experimentally determined rotational correlation time of cyclosporin A (i.e. ~ 0.3 ns) and also the magnitude of structural deviations is small. As shown in Figure 3c, simulations at 298 and 315 K overestimate the rigidity of cyclosporin A; at 490 K, there is better agreement with the results of the NMR spin relaxation analysis. The force field parameters acting on the system at lower temperatures appear to be too restrictive, but this restriction is compensated by increasing the simulation temperature so that the NMR-observed behavior can be better replicated *in silico*. Effectively the high

temperature simulations provide sufficient energy to fast-track the simulations so that dynamics trends can be predicted in a reasonable timeframe and without significantly affecting the thermodynamics of the system.^{34,50} Note that there is no inference that the 490K temperature would ever be reached (or relevant) in a biological system.

Simulations of the open structure of cyclosporin A in chloroform

We attempted to simulate conversion of the open to closed form in chloroform, but this structural conversion was initially difficult to simulate (Figure 4a). We conducted molecular dynamics simulations of the open structure in an explicit chloroform box, but conversion was not observed over the simulated time at 315 K. A higher temperature simulation was better able to induce conversion, giving conformations that were similar to the closed form. These closed form-like conformations differed from the closed conformation mainly by the geometry of the Mle-3 peptide bond, i.e., they were in the *trans*, rather than *cis*, orientation (Figure 4a). Based on this observation, we speculated that the force field parameters acting on the ω -bond angle are overly constraining, so we investigated whether the force field could be modified to allow for *cis/trans* inter-conversion.

We carried out atomic biased force calculations to explore the effect of the peptide bond parameters on the ω -dihedral free energy landscape of a model system comprising a N- and C-capped amino acid and found the *cis/trans* transition energies could be reduced by decreasing the appropriate force constants (Figure 4b). Specifically, a capped Ala residue was subjected to 2.5 ns and 25 ns simulations, both of which had similar energy profiles, suggesting convergence in sampling was obtained. Addition of a methyl group at the amide position, without modifying the force field parameters for the remainder of the amino acid, resulted in an 18% reduction in the transition energy barrier, as well as a 60% reduction in the free energy of the *cis* state. This result is consistent with quantum mechanical calculations on the effect of N-methylation on *cis/trans* conversion of Ac-X-OMe amino acids, reporting an average drop of 80% in the energy difference between the *cis-trans* conformations after N-substitution.⁵¹ Lowering of the force constant of the parameters acting on the ω -dihedral angle in the force field to 80% and then 60%

of the original values resulted in further reductions of the transition free energy, yet maintained the free energy level of the *cis* state.

By incorporating the modified force field tested in the model Ala system into a full simulation for cyclosporin A we identified conditions in which the open structure converted to the closed structure in chloroform (Figure 4c). Initially, reduction of the force constants to 80% of their original values did not improve sampling of the closed structure at 490 K. However, a further reduction of the force constants, to 60% of their original values, improved sampling (Figure 4c). Interconversion between the open and closed structures was observed using the modified force field at 448 K, but not at 315 or 393 K (Figure 4d). Although the closed structure was successfully regenerated from the open structure at both 448 and 490 K, the closed structure did not remain stable for the entire simulation (Figures 4c and d); this is not unexpected as cyclosporin A exchanges between a major and minor conformation in chloroform (Figure 2a) probably due to *cis/trans* isomerization²⁶ as noted above. Modifying only the force field parameters that act on the Mle-3 ω -angle resulted not only in the occurrence of the closed structure, but also in increased structural stability of the closed form (Figure 4d). Overall, the results show that the original force field imposed energetic penalties that inhibited complete conversion of the open to the closed structure within the simulation times. Increasing the temperature and relaxation of the force constants facilitated formation of the closed structure.

Simulations of the open and closed forms of cyclosporin A in water

NMR studies of cyclosporin A indicate that it adopts multiple conformations in water,¹⁰ and we found that this behavior could be replicated *in silico*. In a box of explicit water, significant deviations from the starting structure, either closed or open, were observed at 315 and 490 K (Figure 5a). The higher temperature simulations were better able to produce the expected behavior because of the transition of the Mle-3 peptide bond from the *cis* to *trans* orientation. As shown in Figure 5b, the water environment leads to conformations that have larger solvent-accessible surface areas and more open polar groups than in chloroform. Overall, the simulations in water provide additional support that the modified force field and higher temperatures appropriately replicate experimental cyclosporin's conformational behavior.

Simulating the transition from water to chloroform

Since the focus of this study is the transition of cyclosporin A between different solvent phases, we simulated the peptide in a biphasic system and found that it readily partitioned into the chloroform phase (Figure 6a). Due to its high lipophilicity, cyclosporin A favors the apolar phase of a polar-apolar biphasic system, with log P values of 2–3 in octanol/heptane³⁶ or octanol/isooctane¹⁰ mixtures. We constructed a simulation box comprising an explicit water phase and an explicit chloroform phase and then positioned the open structure of cyclosporin A in the center of the aqueous partition. Cyclosporin A moved rapidly into the chloroform partition and then remained just under the chloroform–water interface for the remainder of the simulation. Cyclosporin A adopted the closed conformation during transition from the upper chloroform–water interface to the lower interface (Figure 6a). We speculated that it was unable to move back through the chloroform phase into the upper interface in the simulation because the interfacial environment did not encourage formation of the closed structure. Indeed, when cyclosporin A was constrained into the closed form, it diffused through the chloroform phase with higher frequency (Figure 6b). On the other hand, when constrained into the open form, it was unable to transition through the chloroform phase and was trapped at the upper water–chloroform interface (Figure 6b). These simulations support the importance of conformational change for the movement of cyclosporin A between different solvent environments.

NMR structural studies of cyclosporin A in membrane mimics

We next altered our focus from chloroform to systems that mimic the membrane environment, and demonstrated that the closed conformation or one similar to that exists in lipids (Figure 7a). We considered cyclohexane because of the abundance of CH₂ groups in both cyclohexane and lipid tails. Additionally, the force field parameters for cyclohexane and lipid tails have many similarities, allowing for more meaningful comparisons between experiment and simulation. We also examined dodecylphosphocholine (DPC) because of its structural similarity to POPC; another approach is to use bicelles. The structure of cyclosporin A in SDS has been previously reported.²⁹ As shown in Figure 7a, the H α chemical shifts show a similar trend across the sequence of cyclosporin A in chloroform, cyclohexane, SDS,²⁹ and DPC, with those in

cyclohexane and chloroform being most similar. Notably, there are some differences in chemical shifts (Figure 7a); for example, Sar-7 exhibits an H α chemical shift in the presence of DPC that is 0.26 ppm downfield to that in chloroform, which might indicate differences in the local backbone geometry. Therefore, the analysis of H α chemical shifts suggest that the conformational behavior of cyclosporin A in DPC is not identical to that in chloroform but could also have similarities.

Figure 7b shows that cyclosporin A adopts a single conformation (or multiple conformations in fast exchange) in cyclohexane. The ^1H 1D spectrum at 288 K (and other temperatures) exhibits four sharp peaks in the amide region that correspond to the four backbone amides, resembling the behavior in chloroform (Figure 2). By comparison, there is greater conformational heterogeneity in the presence of DPC because of the presence of slow-exchanging conformations in addition to the major conformer. The distribution of these peaks in the ^1H 1D spectrum as well as the H α chemical shifts of the main conformer did not change significantly as the cyclosporin to DPC ratio was increased from 1:50 to 1:100 (Supplementary Table S1, Supplementary Figures S1–S4). Despite these differences in the ^1H 1D spectrum between chloroform and DPC, preliminary structures of cyclosporin A at 1:50 and 1:100 peptide to DPC ratios calculated using NOE restraints (Supplementary Tables S2 and S3, Supplementary Figures S5 and S6) indicate that the structure in DPC could resemble the closed conformation, although there might be differences in the backbone geometry, for example at Sar-7 and Ala-11 (Supplementary Figure S7). Similarity in the general trend in temperature coefficients and $^3J_{\text{HN-H}\alpha}$ constants (Supplementary Table S4) with the presence of localized differences (e.g. Ala-11 having ~ 1 Hz $^3J_{\text{HN-H}\alpha}$ difference between cyclohexane and DPC) supports this conclusion. Although the structures could be further refined, the data generally show that the closed form could exist in a lipid bilayer.

Simulations of cyclosporin A in cyclohexane

We next showed that cyclosporin A could adopt the closed structure in cyclohexane *in silico* (Figure 8a). We placed the open form of cyclosporin A in a box of explicit cyclohexane and

carried out molecular dynamics simulations. At 315 K, the simulated structures did not approach the closed form, but increasing the temperature improved sampling of the closed structure. At 448 K, for example, the open structure rapidly converted to the closed form and remained stable in the closed structure. A further increase in temperature to 490 K resulted in sampling of additional non-closed structures, so 448 K was the optimal simulation temperature.

Simulations of cyclosporin A with a lipid bilayer

Having characterized the behavior of cyclosporin A in various solvent environments and with different simulation parameters, we conducted simulations of cyclosporin A in the presence of a lipid bilayer, and found that conformational dynamics is an important determinant of permeability (Figure 8b–f). A simulation box comprising a POPC lipid bilayer patch and the open structure of cyclosporin A positioned above the patch was constructed. Early in the simulation, cyclosporin A partitioned into the lipid bilayer (Figure 8b). We experimentally confirmed that cyclosporin A can bind to a POPC lipid bilayer using SPR with the bilayer deposited on a L1 sensor chip, as shown in Supplementary Figure S8. Over the course of the simulation, cyclosporin A moved through the lipid bilayer while adopting various conformations, including the closed form. Solid-state NMR and small angle X-ray diffraction experiments have previously shown that cyclosporin A can reside in the membrane interior.⁵² Figure 8c shows that the closed form is preferred when cyclosporin A is sequestered near the lipid tails where there is low exposure to water, but becomes less preferred as cyclosporin A moves away from the membrane core and becomes more open to water.

We then examined the effect of temperature on the translational properties of cyclosporin A *in silico* (Figure 8d). At 315 K, cyclosporin A remains in the aqueous phase. At 393 K, it enters the membrane but is stuck in the upper leaflet of the bilayer. At both 315 and 393 K, the closed structure is never observed. At 490 K, cyclosporin A is again able to move through the lipid bilayer, but the movement is more rapid and the occurrence of the closed structure is less frequent compared to the simulation at 448 K. A change in the simulation temperature also affects the lipid bilayer. Figure 8e shows that an increase in temperature results in thinning of the bilayer, as indicated by increases in the area per lipid. Thus, the ability of cyclosporin A to move

through the bilayer could be due to the ability of the simulated structures to adopt the closed form and/or porosity of the lipid bilayer.

To explore whether the conformation of cyclosporin A is indeed a determinant of its membrane permeability in the presence of a thinned bilayer, simulations of cyclosporin A constrained in either the closed form or the open form were carried out and compared to simulations without constraints. As shown in Figure 8f, when cyclosporin A is not constrained, its distance from the membrane center is distributed along the normal of the bilayer. When cyclosporin A is constrained in the closed form, the distance distribution is narrower because it predominantly stays in a lipid core surrounded by lipid tails. When cyclosporin A is constrained in the open conformation, it is unable to permeate the membrane and remains trapped in the upper leaflet. Overall, the simulations of cyclosporin A, either unconstrained or constrained, show that conformational flexibility is important for the membrane permeability of cyclosporin A.

Extension to simulations of cyclosporin H and other cyclic hexapeptides in a lipid bilayer

To provide further validation and to broaden the study, we conducted simulations of other cyclic peptides, including cyclosporin H (Figure 9a) and two cyclic hexapeptides (Figure 9b), in the presence of a lipid bilayer, and confirmed that conformational flexibility can indeed affect movement through a membrane. Cyclosporin H is able to passively diffuse across an artificial membrane, but is less permeable than cyclosporin A (i.e. $\log(P_e)$ of -5.36 compared to -5.01).¹¹ It differs from cyclosporin A by a stereochemical inversion at residue 4, but like cyclosporin A, it also exhibits solvent-dependent conformational change (Figure 9a). Its solid-state structure has been determined from methanol-grown crystals (Figure 9a);⁴² however, the structure is different to those reported for cyclosporin A (Figure 1), and so provides a different starting point for our *in silico* investigations. As shown in Figure 9c, when cyclosporin H starts (unconstrained) in this conformation in the presence of a membrane, it enters the membrane and transitions to the other side, sampling different locations along the membrane normal during the simulation, including the membrane core and the outer aqueous compartment. By comparison, when constrained in this starting conformation, cyclosporin H rapidly partitions into the membrane, but does not sample as diverse a range of locations. A similar dependence of positional distribution on

conformational restriction is also exhibited by a cyclic hexapeptide (i.e. cyclic peptide 13) that we have previously shown to have high passive membrane permeability and oral bioavailability (i.e., $F = 33\%$ when administered orally in rats).¹⁶ The unconstrained peptide moves more freely through the membrane than its constrained form or a non-N-methylated variant (i.e. cyclic peptide 1, which was first reported as compound 4²⁴) reported to have lower permeability.¹⁶ Overall, the simulation results clearly demonstrate that conformational flexibility can help mediate passive transport across membranes.

Discussion

Here we studied how conformational dynamics affects the passage of peptides across biological membranes. We focused on cyclosporin A, a peptide drug that has high membrane permeability for its size.¹⁹ Its conformational flexibility has been hypothesized to be a key determinant of its ability to cross membranes.^{11,23,24} This hypothesis has been difficult to study, particularly at the molecular level, because the factors that affect permeability are multifarious and many biophysical techniques lack the spatial and temporal resolution needed. Thus, we explored the potential of molecular dynamics, alongside NMR, to characterize the dynamics of cyclosporin A and other membrane permeable cyclic peptides, and their spontaneous partitioning into and out of lipid membranes.

Studying membrane permeability of cyclosporin A using molecular dynamics is challenging because membrane diffusion and conformational change, including *cis*–*trans* bond transitions, occur on slow timescales. Specifically, based on an apparent permeability of $\sim 10^{-5}$ cm/s,¹¹ the rate at which cyclosporine A crosses a lipid bilayer would be ~ 10 s⁻¹. Compared to this, *cis*–*trans* rotation about the Mle-2 peptide bond is slower in an aqueous-like environment (i.e. $\sim 10^{-3}$ s⁻¹ in pure tetrahydrofuran⁵³). In chloroform, the interconversion rate increases by up to 1000-fold, with a *cis* to *trans* conversion rate of $\sim 10^{-2}$ s⁻¹ and *trans* to *cis* conversion of 1 s⁻¹; these rates further increase with increasing temperature.⁵⁴ Clearly, the timescale of these processes require substantial computational resources and/or advanced sampling techniques for exhaustive characterization. Indeed, previous molecular dynamics simulations have been too short (i.e., 50 ps–2.1 ns) to observe conformational changes at ambient temperatures without adding biased restraints.^{35,37} Longer simulations (i.e., 100 ns seeded simulations; 10 μ s total) at near ambient temperatures have demonstrated more success in obtaining convergence, showing that expected behavior (e.g., *cis*–*trans* bond populations) can be simulated.³⁸

Our approach was to perform simulations using a wide range of conditions (i.e, at a range of temperatures, in a range of solvents, using a range of structural parameters), and to interpret the results with reference to NMR data. As in previous simulations, elevated temperatures were used to accelerate sampling.^{33,34,37} The use of high temperatures in simulations is now widespread, and

has proved valuable to study peptide–membrane interactions. For example, the partitioning and transmembrane insertion of helical polyleucine segments have been studied at 353–490 K, which directly revealed all states populated at equilibrium.³³ Here, we demonstrated that elevated temperatures indeed improved sampling and produced better agreement with experimental results compared to lower temperature simulations. For example, elevated temperature simulations of the open structure in either chloroform or cyclohexane facilitated conversion into the closed form, consistent with experimental observations (Figures 1 and 7b). Furthermore, there was a higher degree of structural deviation in chloroform compared to cyclohexane, again confirmed by experimental data (Figures 1 and 7b). As well as elevated temperatures, which facilitates peptide bond isomerization *in silico*,⁵⁵ modification of the force field parameters acting on the ω -angle of N-methylated residues also assisted in improving sampling (Figure 4c). Nevertheless, the requirement of higher temperatures and force field modifications suggest that large energy barriers restrict sampling in the system studied here. With modifications to the simulation parameters, we confirmed the dependence of conformation on the solvent observed experimentally.^{10,25-29} By performing simulations in simple solvent systems first, we established a foundation for studying cyclosporin A in the presence of lipid bilayers.

Cyclosporin A permeates membranes in *in vitro* trans-well assays,^{10,11} confirming that passive diffusion across membranes is an important step towards achieving cell permeability and oral absorption. We aimed to address the question of whether conformational flexibility is important for this membrane permeability. The observation that unconstrained cyclosporin A can move more freely in a water–chloroform biphasic system than can either the constrained closed or open structures provided initial evidence in support of the importance of dynamics (Figure 6b). Further support came from simulations in the presence of a lipid bilayer (Figure 8f). Unconstrained cyclosporin A moved more freely in a lipid bilayer than constrained cyclosporin A, which was predominantly trapped in the membrane core or interface depending, on whether it was in the closed or open structure, respectively. Additionally, this dependence of movement through a lipid bilayer on conformational flexibility was observed for other cyclic peptides reported to be membrane permeable (Figure 9). If complete rigidity can limit permeability, does this mean that flexibility is the key? To a degree. Increased flexibility, for example as would

occur by linearizing cyclosporin A, would be expected to decrease permeability because the linear peptide would be less able to sample the conformation favorable for membrane insertion.

Conformational polymorphism affects all stages of the membrane permeability of cyclosporin A (Figure 10). To permeate membranes, cyclosporin A must transition from an aqueous environment into the chemically-opposing environment of the membrane core. Based on studies of membrane permeability of peptides,^{19,20,56} many factors are thought to affect this transition, including electrostatic contributions, non-polar contributions, and lipid perturbation effects, in addition to peptide conformational effects. In the aqueous phase, cyclosporin A samples multiple conformations as evidenced by 1D ¹H NMR spectra in polar solvents and water.^{10,27} In water, both closed and open conformations are not stable *in silico*; however, these starting conformations may still exist sporadically, as previously suggested.³⁸ Some of the conformations sampled in water are more favorable than others for insertion into as well as movement through the membrane. For example, although both the closed and open form can partition to the membrane *in silico*, only the closed form can more freely move through the membrane; the open form prefers to sit at the water–membrane interface (Figure 8). The inter-conversion rates between conformations that favor and disfavor membrane permeability are thought to drive permeability, particularly when the time scales of conversion are slower than permeation.³⁹

On average, insertion of cyclosporin A into a lipid membrane is an endothermic process, governed by an enthalpic penalty that is counterbalanced by favorable entropic changes.⁵² The enthalpic contribution to insertion might be brought about by: (i) a reordering of water molecules about the peptide surface; (ii) changes in hydrogen bonding between water and cyclosporin A; or, (iii) a combination of both processes. Evidence of multiple conformations of cyclosporin A, in which some have smaller polar surface areas or have their backbone polar groups more protected from the solvent, supports the role of conformational change in facilitating insertion. Additionally, some conformations of cyclosporin A have larger non-polar surface areas, which would facilitate insertion via the classical hydrophobic effect, which is an entropy-driven phenomenon. Both electrostatic and non-polar contributions add to the overall desolvation energy, which has been suggested to be a predictor of membrane permeability.^{12,23}

Upon insertion into a membrane, cyclosporin A can partition into the membrane core.^{52,57} Based on structural studies in chloroform (a solvent with a low dielectric constant that mimics the membrane core), cyclosporin A is commonly assumed to adopt the closed structure inside the membrane. We showed using a NMR relaxation analysis that cyclosporin A exhibits limited amplitude fast backbone motion; we hypothesize that the lack of absolute rigidity is important to enable structural change. We further demonstrated that cyclosporin A can indeed form the closed form in environments that mimic the membrane (Figure 7a); for example, the H α chemical shifts of cyclosporin A in cyclohexane are almost identical to those in chloroform. In the presence of DPC, the chemical shifts are, generally, similar to those in cyclohexane and chloroform, suggesting that the overall structure in the micelle environment resembles the closed form. This conclusion is supported by a comparison of temperature-dependent amide proton shifts (markers of solvent exposure and hydrogen bonding) in cyclohexane with those in the presence of DPC. We demonstrated that the closed structure favored the membrane interior when cyclosporin A was constrained during simulations in the presence of a lipid bilayer (Figure 8f). However, when cyclosporin A was not constrained, alternative conformations were observed in the membrane core. Conformational flexibility might be beneficial inside the membrane because it might reduce the entropic cost of insertion. It also increases sampling of positions along the membrane normal (Figure 8f), suggesting that it might also facilitate departure of cyclosporin A from the membrane interior, as was observed for cyclosporin H and cyclic peptide 13 (Figure 9c).

It is also thought that lipid perturbation effects can affect membrane insertion of peptides. Lipid perturbation effects arise from conformational dynamics of the lipid chains in the bilayer and are dependent on the size of the inserted peptide. We observed that changes in the conformation of cyclosporin A resulted in changes in the overall size, with the closed conformation being generally smaller than those found in water (Figure 5b). Peptide size also affects diffusion of a peptide through a membrane, as corroborated in a recent study of a range of cyclic peptides.¹⁹ As that study noted, as did an earlier study,⁵⁸ diffusion through a membrane is in accord with a polymer-based model rather than a Stokes-Einstein model. In the polymer model, peptides move through the membrane by successively occupying nearby voids that sporadically appear. This

might explain the observation that insertion is favored in elevated temperature simulations, in which the membrane is less compact (Figure 8). Interestingly, the polymer-model predicts that the diffusion rate correlates with the short dimension of the diffusant; this is consistent with the closed conformation being favorable for membrane permeation because it resembles an elongated shape with one dimension shorter than the other (Figure 1). If the polymer model is more appropriate for representing membrane permeability, then simulations in the presence of a lipid bilayer should have broad utility for studying peptide permeability.

Conclusions

In summary, we have used simulations to provide a molecular microscope to monitor the dynamics of membrane-permeable cyclic peptides and its role in membrane permeability. We found that conformational polymorphism is indeed an important feature of these peptides, allowing them to more readily move through a lipid bilayer. Given that increasing attention is being paid to exploring the potential of peptides as therapeutics, there is a greater need to understand how peptides can permeate membranes, leading to a better understanding of how peptides might be modified so that they can be delivered orally.

Supporting Information

- $H\alpha$ chemical shifts of cyclosporin A in the presence of DPC.
- NOE analysis of cyclosporin A in the presence of DPC.
- Amide temperature coefficients and coupling constants of cyclosporin A in cyclohexane and in the presence of DPC.
- TOCSY and NOESY spectra of cyclosporin A in the presence of DPC.
- Structural statistics of cyclosporin A structures
- Solution structures of cyclosporin A in the presence of DPC.
- SPR analysis of cyclosporin binding to POPC lipid bilayers.

Acknowledgements

DJC is an Australian Research Council (ARC) Australian Laureate (FL150100146) and JES is a National Health and Medical Research Council (NHMRC) Early Career Fellow (APP1069819). Work in our laboratory on peptide scaffolds is supported by grants from the ARC (DP150100443) and the NHMRC (APP1107403). We thank Ashley Cooper for proofreading and editorial assistance.

References

- (1) Craik, D. J.; Fairlie, D. P.; Liras, S.; Price, D. The Future of Peptide-Based Drugs. *Chem Biol Drug Des* **2013**, *81*, 136-147.
- (2) Kawamura, A.; Munzel, M.; Kojima, T.; Yapp, C.; Bhushan, B.; Goto, Y.; Tumber, A.; Katoh, T.; King, O. N.; Passioura, T. *et al.* Highly Selective Inhibition of Histone Demethylases by De Novo Macrocyclic Peptides. *Nat Commun* **2017**, *8*, 14773.
- (3) Cox, N.; Kintzing, J. R.; Smith, M.; Grant, G. A.; Cochran, J. R. Integrin-Targeting Knottin Peptide-Drug Conjugates Are Potent Inhibitors of Tumor Cell Proliferation. *Angew Chem Int Ed Engl* **2016**, *55*, 9894-9897.
- (4) Maltsev, O. V.; Marelli, U. K.; Kapp, T. G.; Di Leva, F. S.; Di Maro, S.; Nieberler, M.; Reuning, U.; Schwaiger, M.; Novellino, E.; Marinelli, L. *et al.* Stable Peptides Instead of Stapled Peptides: Highly Potent Alphavbeta6-Selective Integrin Ligands. *Angew Chem Int Ed Engl* **2016**, *55*, 1535-1539.
- (5) Chen, S.; Gopalakrishnan, R.; Schaer, T.; Marger, F.; Hovius, R.; Bertrand, D.; Pojer, F.; Heinis, C. Dithiol Amino Acids Can Structurally Shape and Enhance the Ligand-Binding Properties of Polypeptides. *Nat Chem* **2014**, *6*, 1009-1016.
- (6) Beveridge, T.; Gratwohl, A.; Michot, F.; Niederberger, W.; Nüesch, E.; Nussbaumer, K.; Schaub, P.; Speck, B. Cyclosporin A: Pharmacokinetics Alter a Single Dose in Man and Serum Levels after Multiple Dosing in Recipients of Allogenic Bone Marrow Grafts. *Curr Ther Res Clin Exp* **1981**, *30*, 5-18.
- (7) Stahelin, H. F. The History of Cyclosporin a (Sandimmune) Revisited: Another Point of View. *Experientia* **1996**, *52*, 5-13.
- (8) Borel, J. F. History of the Discovery of Cyclosporin and of Its Early Pharmacological Development. *Wien Klin Wochenschr* **2002**, *114*, 433-437.
- (9) Matsuda, S.; Koyasu, S. Mechanisms of Action of Cyclosporine. *Immunopharmacology* **2000**, *47*, 119-125.
- (10) Augustijns, P. F.; Brown, S. C.; Willard, D. H.; Consler, T. G.; Annaert, P. P.; Hendren, R. W.; Bradshaw, T. P. Hydration Changes Implicated in the Remarkable Temperature-Dependent Membrane Permeation of Cyclosporin A. *Biochemistry* **2000**, *39*, 7621-7630.
- (11) Ahlbach, C. L.; Lexa, K. W.; Bockus, A. T.; Chen, V.; Crews, P.; Jacobson, M. P.; Lokey, R. S. Beyond Cyclosporine A: Conformation-Dependent Passive Membrane Permeabilities of Cyclic Peptide Natural Products. *Future Med Chem* **2015**, *7*, 2121-2130.
- (12) Conradi, R. A.; Hilgers, A. R.; Ho, N. F.; Burton, P. S. The Influence of Peptide Structure on Transport across Caco-2 Cells. *Pharm Res* **1991**, *8*, 1453-1460.
- (13) Okumu, F. W.; Pauletti, G. M.; Vander Velde, D. G.; Siahaan, T. J.; Borchardt, R. T. Effect of Restricted Conformational Flexibility on the Permeation of Model Hexapeptides across Caco-2 Cell Monolayers. *Pharm Res* **1997**, *14*, 169-175.

- (14) Biron, E.; Chatterjee, J.; Ovadia, O.; Langenegger, D.; Brueggen, J.; Hoyer, D.; Schmid, H. A.; Jelinek, R.; Gilon, C.; Hoffman, A.*et al.* Improving Oral Bioavailability of Peptides by Multiple N-Methylation: Somatostatin Analogues. *Angew Chem Int Ed Engl* **2008**, *47*, 2595-2599.
- (15) White, T. R.; Renzelman, C. M.; Rand, A. C.; Rezai, T.; McEwen, C. M.; Gelev, V. M.; Turner, R. A.; Linington, R. G.; Leung, S. S.; Kalgutkar, A. S.*et al.* On-Resin N-Methylation of Cyclic Peptides for Discovery of Orally Bioavailable Scaffolds. *Nat Chem Biol* **2011**, *7*, 810-817.
- (16) Wang, C. K.; Northfield, S. E.; Colless, B.; Chaousis, S.; Hamernig, I.; Lohman, R. J.; Nielsen, D.; Schroeder, C. I.; Liras, S.; Price, D. A.*et al.* Rational Design and Synthesis of Orally Bioavailable Peptides Directed by Nmr Amide Temperature Coefficients. *Proc Natl Acad Sci* **2014**, *111*, 17504-17509.
- (17) Rand, A. C.; Leung, S. S.; Eng, H.; Rotter, C. J.; Sharma, R.; Kalgutkar, A. S.; Zhang, Y.; Varma, M. V.; Farley, K. A.; Khunte, B.*et al.* Optimizing Pk Properties of Cyclic Peptides: The Effect of Side Chain Substitutions on Permeability and Clearance(). *Medchemcomm* **2012**, *3*, 1282-1289.
- (18) Beck, J. G.; Chatterjee, J.; Laufer, B.; Kiran, M. U.; Frank, A. O.; Neubauer, S.; Ovadia, O.; Greenberg, S.; Gilon, C.; Hoffman, A.*et al.* Intestinal Permeability of Cyclic Peptides: Common Key Backbone Motifs Identified. *J Am Chem Soc* **2012**, *134*, 12125-12133.
- (19) Pye, C. R.; Hewitt, W. M.; Schwochert, J.; Haddad, T. D.; Townsend, C. E.; Etienne, L.; Lao, Y.; Limberakis, C.; Furukawa, A.; Mathiowetz, A. M.*et al.* Nonclassical Size Dependence of Permeation Defines Bounds for Passive Adsorption of Large Drug Molecules. *J Med Chem* **2017**, *60*, 1665-1672.
- (20) Leung, S. S.; Sindhikara, D.; Jacobson, M. P. Simple Predictive Models of Passive Membrane Permeability Incorporating Size-Dependent Membrane-Water Partition. *J Chem Inf Model* **2016**, *56*, 924-929.
- (21) Naylor, M. R.; Bockus, A. T.; Blanco, M. J.; Lokey, R. S. Cyclic Peptide Natural Products Chart the Frontier of Oral Bioavailability in the Pursuit of Undruggable Targets. *Curr Opin Chem Biol* **2017**, *38*, 141-147.
- (22) Bockus, A. T.; Lexa, K. W.; Pye, C. R.; Kalgutkar, A. S.; Gardner, J. W.; Hund, K. C.; Hewitt, W. M.; Schwochert, J. A.; Glassey, E.; Price, D. A.*et al.* Probing the Physicochemical Boundaries of Cell Permeability and Oral Bioavailability in Lipophilic Macrocycles Inspired by Natural Products. *J Med Chem* **2015**, *58*, 4581-4589.
- (23) Rezai, T.; Bock, J. E.; Zhou, M. V.; Kalyanaraman, C.; Lokey, R. S.; Jacobson, M. P. Conformational Flexibility, Internal Hydrogen Bonding, and Passive Membrane Permeability: Successful in Silico Prediction of the Relative Permeabilities of Cyclic Peptides. *J Am Chem Soc* **2006**, *128*, 14073-14080.
- (24) Rezai, T.; Yu, B.; Millhauser, G. L.; Jacobson, M. P.; Lokey, R. S. Testing the Conformational Hypothesis of Passive Membrane Permeability Using Synthetic Cyclic Peptide Diastereomers. *J Am Chem Soc* **2006**, *128*, 2510-2511.
- (25) Loosli, H. R.; Kessler, H.; Oschkinat, H.; Weber, H. P.; Petcher, T. J.; Widmer, A. Peptide Conformations. Part 31. The Conformation of Cyclosporin a in the Crystal and in Solution. *Helv Chim Acta* **1985**, *68*, 682-704.

- (26) Kessler, H.; Köck, M.; Wein, T.; Gehrke, M. Reinvestigation of the Conformation of Cyclosporin a in Chloroform. *Helv Chim Acta* **1990**, *73*, 1818-1832.
- (27) Ko, S. Y.; Dalvit, C. Conformation of Cyclosporin a in Polar Solvents. *Int J Pept Protein Res* **1992**, *40*, 380-382.
- (28) Bernardi, F.; Gaggelli, E.; Molteni, E.; Porciatti, E.; Valensin, D.; Valensin, G. ¹h and ¹³c-Nmr and Molecular Dynamics Studies of Cyclosporin a Interacting with Magnesium(II) or Cerium(III) in Acetonitrile. Conformational Changes and Cis-Trans Conversion of Peptide Bonds. *Biophys J* **2006**, *90*, 1350-1361.
- (29) Bernardi, F.; D'Amelio, N.; Gaggelli, E.; Molteni, E.; Valensin, G. Solution Structures of Cyclosporin a and Its Complex with Dysprosium(III) in Sds Micelles: Nmr and Molecular Dynamics Studies. *J Phys Chem B* **2008**, *112*, 828-835.
- (30) Theriault, Y.; Logan, T. M.; Meadows, R.; Yu, L.; Olejniczak, E. T.; Holzman, T. F.; Simmer, R. L.; Fesik, S. W. Solution Structure of the Cyclosporin a/Cyclophilin Complex by Nmr. *Nature* **1993**, *361*, 88-91.
- (31) Kallen, J.; Mikol, V.; Taylor, P.; Walkinshaw, M. D. X-Ray Structures and Analysis of 11 Cyclosporin Derivatives Complexed with Cyclophilin A. *J Mol Biol* **1998**, *283*, 435-449.
- (32) Wenger, R. M.; France, J.; Bovermann, G.; Walliser, L.; Widmer, A.; Widmer, H. The 3d Structure of a Cyclosporin Analogue in Water Is Nearly Identical to the Cyclophilin-Bound Cyclosporin Conformation. *FEBS Lett* **1994**, *340*, 255-259.
- (33) Ulmschneider, J. P.; Smith, J. C.; White, S. H.; Ulmschneider, M. B. In Silico Partitioning and Transmembrane Insertion of Hydrophobic Peptides under Equilibrium Conditions. *J Am Chem Soc* **2011**, *133*, 15487-15495.
- (34) Ulmschneider, M. B.; Ulmschneider, J. P.; Schiller, N.; Wallace, B. A.; von Heijne, G.; White, S. H. Spontaneous Transmembrane Helix Insertion Thermodynamically Mimics Translocon-Guided Insertion. *Nat Commun* **2014**, *5*, 4863.
- (35) Lautz, J.; Kessler, H.; van Gunsteren, W. F.; Weber, H. P.; Wenger, R. M. On the Dependence of Molecular Conformation on the Type of Solvent Environment: A Molecular Dynamics Study of Cyclosporin A. *Biopolymers* **1990**, *29*, 1669-1687.
- (36) el Tayar, N.; Mark, A. E.; Vallat, P.; Brunne, R. M.; Testa, B.; van Gunsteren, W. F. Solvent-Dependent Conformation and Hydrogen-Bonding Capacity of Cyclosporin A: Evidence from Partition Coefficients and Molecular Dynamics Simulations. *J Med Chem* **1993**, *36*, 3757-3764.
- (37) O'Donohue, M. F.; Burgess, A. W.; Walkinshaw, M. D.; Treutlein, H. R. Modeling Conformational Changes in Cyclosporin A. *Protein Sci* **1995**, *4*, 2191-2202.
- (38) Witek, J.; Keller, B. G.; Blatter, M.; Meissner, A.; Wagner, T.; Riniker, S. Kinetic Models of Cyclosporin a in Polar and Apolar Environments Reveal Multiple Congruent Conformational States. *J Chem Inf Model* **2016**, *56*, 1547-1562.

- (39) Witek, J.; Muhlbauer, M.; Keller, B. G.; Blatter, M.; Meissner, A.; Wagner, T.; Riniker, S. Interconversion Rates between Conformational States as Rationale for the Membrane Permeability of Cyclosporines. *Chemphyschem* **2017**, *18*, 3309-3314.
- (40) Vranken, W. F.; Boucher, W.; Stevens, T. J.; Fogh, R. H.; Pajon, A.; Llinas, M.; Ulrich, E. L.; Markley, J. L.; Ionides, J.; Laue, E. D. The Ccpn Data Model for Nmr Spectroscopy: Development of a Software Pipeline. *Proteins* **2005**, *59*, 687-696.
- (41) Wang, C. K.; Swedberg, J. E.; Northfield, S. E.; Craik, D. J. Effects of Cyclization on Peptide Backbone Dynamics. *J Phys Chem B* **2015**, *119*, 15821-15830.
- (42) Potter, B.; Palmer, R. A.; Withnall, R.; Jenkins, T. C.; Chowdhry, B. Z. Two New Cyclosporin Folds Observed in the Structures of the Immunosuppressant Cyclosporin G and the Formyl Peptide Receptor Antagonist Cyclosporin H at Ultra-High Resolution. *Org Biomol Chem* **2003**, *1*, 1466-1474.
- (43) Dietz, W.; Heinzinger, K. A Molecular Dynamics Study of Liquid Chloroform. *Ber Bunsen-Ges Phys Chem* **1985**, *89*, 968-977.
- (44) Yu, W.; He, X.; Vanommeslaeghe, K.; MacKerell, A. D., Jr. Extension of the Charmm General Force Field to Sulfonyl-Containing Compounds and Its Utility in Biomolecular Simulations. *J Comput Chem* **2012**, *33*, 2451-2468.
- (45) Wang, C. K.; Northfield, S. E.; Swedberg, J. E.; Colless, B.; Chaousis, S.; Price, D. A.; Liras, S.; Craik, D. J. Exploring Experimental and Computational Markers of Cyclic Peptides: Charting Islands of Permeability. *Eur J Med Chem* **2015**, *97*, 202-213.
- (46) Kasinath, V.; Sharp, K. A.; Wand, A. J. Microscopic Insights into the Nmr Relaxation-Based Protein Conformational Entropy Meter. *J Am Chem Soc* **2013**, *135*, 15092-15100.
- (47) Lipari, G.; Szabo, A. Model-Free Approach to the Interpretation of Nuclear Magnetic Resonance Relaxation in Macromolecules. I. Theory and Range of Validity. *J Am Chem Soc* **1982**, *104*, 4546-4559.
- (48) Dellwo, M. J.; Wand, A. J. Model-Independent and Model-Dependent Analysis of the Global and Internal Dynamics of Cyclosporin A. *J Am Chem Soc* **1989**, *111*, 4571-4578.
- (49) Conibear, A. C.; Wang, C. K.; Bi, T.; Rosengren, K. J.; Camarero, J. A.; Craik, D. J. Insights into the Molecular Flexibility of Theta-Defensins by Nmr Relaxation Analysis. *J Phys Chem B* **2014**, *118*, 14257-14266.
- (50) Wang, Y.; Chen, C. H.; Hu, D.; Ulmschneider, M. B.; Ulmschneider, J. P. Spontaneous Formation of Structurally Diverse Membrane Channel Architectures from a Single Antimicrobial Peptide. *Nat Commun* **2016**, *7*, 13535.
- (51) Md Abdur Rauf, S.; Arvidsson, P. I.; Albericio, F.; Govender, T.; Maguire, G. E.; Kruger, H. G.; Honarparvar, B. The Effect of N-Methylation of Amino Acids (Ac-X-Ome) on Solubility and Conformation: A Dft Study. *Org Biomol Chem* **2015**, *13*, 9993-10006.

- (52) Schote, U.; Ganz, P.; Fahr, A.; Seelig, J. Interactions of Cyclosporines with Lipid Membranes as Studied by Solid-State Nuclear Magnetic Resonance Spectroscopy and High-Sensitivity Titration Calorimetry. *J Pharm Sci* **2002**, *91*, 856-867.
- (53) Kofron, J. L.; Kuzmic, P.; Kishore, V.; Gemmecker, G.; Fesik, S. W.; Rich, D. H. Lithium Chloride Perturbation of Cis-Trans Peptide Bond Equilibria: Effect on Conformational Equilibria in Cyclosporin a and on Time-Dependent Inhibition of Cyclophilin. *J Am Chem Soc* **1992**, *114*, 2670-2675.
- (54) Efimov, S. V.; Karataeva, F. K.; Aganov, A. V.; Berger, S.; Klochkov, V. V. Spatial Structure of Cyclosporin a and Insight into Its Flexibility. *J Mol Struct* **2016**, *1036*, 298-304.
- (55) Neale, C.; Pomes, R.; Garcia, A. E. Peptide Bond Isomerization in High-Temperature Simulations. *J Chem Theory Comput* **2016**, *12*, 1989-1999.
- (56) Wang, C. K.; Craik, D. J. Cyclic Peptide Oral Bioavailability: Lessons from the Past. *Biopolymers* **2016**, *106*, 901-909.
- (57) Lambros, M. P.; Rahman, Y. E. Effects of Cyclosporin a on Model Lipid Membranes. *Chem Phys Lipids* **2004**, *131*, 63-69.
- (58) Lieb, W. R.; Stein, W. D. Implications of Two Different Types of Diffusion for Biological Membranes. *Nat New Biol* **1971**, *234*, 220-222.

Figure Legends

Figure 1. Cyclosporin A, open and closed structures, and the question of membrane permeability. The sequence and chemical structure of cyclosporin A is shown at the top right, with each residue labelled with its three-letter code. Residues 1, 5, and 10 are labelled with the residue number. Cyclosporin A has seven N-methylated amino acids (i.e., Mle-2, Mle-3, Mva-4, Bmt-5, Sar-7, Mle-8, and Mle-10) and four non-N-methylated amino acids (i.e., Dal-1, Aba-6, Val-9, and Ala-11). It has a cyclic backbone, as indicated by the black line connecting the last residue to the first. Based on reported structures, the peptide bond between Mle-2 and Mle-3 can adopt either a *cis* or *trans* conformations. Structures of cyclosporin A bound to a protein target (typically cyclophilin) are similar (blue, only backbone shown for clarity; top left), and have the Mle-3 bond in the *trans* orientation. We have chosen one of these to represent the 'open' conformation. In chloroform, cyclosporin A adopts an extended conformation (orange) in which the Mle-3 bond adopts a *cis* orientation. We refer to this structure as the 'closed' conformation. A schematic of a lipid bilayer is shown to highlight the overall focus of the manuscript on membrane permeability.

Figure 2. Dynamics of cyclosporin A characterized by NMR. **a)** ^1H 1D NMR spectra of cyclosporin A in various solvents, including aqueous mixtures of deuterated acetonitrile and water (38–100% v/v CD_3CN), and pure deuterated chloroform (CDCl_3). The sample temperature as well as the solvent composition is shown to the left of each spectrum. The four backbone amides of cyclosporin A are labelled. The asterisk indicates the solvent peak. **b)** ^{13}C Spin-lattice (T_1) and heteronuclear NOE (hNOE) values recorded at 500, 600, and 900 MHz in CDCl_3 at 298 K, and were used to derive generalized order parameters (S^2) from a model-free analysis. The sequence of the cyclosporin A is shown for reference.

Figure 3. Molecular dynamics simulations of the closed structure in chloroform. Simulations in explicit chloroform were carried out using the closed structure as the starting point. **a)** Root mean squared deviation (RMSD; backbone heavy atoms) of simulated structures compared to the closed structure at 298, 315, and 490 K. **b)** The conformations at two time-points in the 490 K simulation, labelled with (i) and (ii), are shown, along with the RMSD

values. **c)** Average order parameters $\langle S^2 \rangle$ were calculated from the simulations and compared to that from the nuclear spin relaxation (NSR) analysis (Figure 2).

Figure 4. Molecular dynamics simulations of the open structure in chloroform. Simulations in explicit chloroform were carried out using the open structure as the starting point. **a)** Root mean squared deviation (RMSD; backbone heavy atoms) of simulated structures compared to the closed structure at 315 and 490 K. The structure at the (i) time-point (green) is aligned to the closed structure (orange). The Mle-3 peptide bond adopts a *trans* orientation, whereas the same bond adopts a *cis* orientation in the closed structure. **b)** Adaptive biasing force calculations of amino acids capped at both terminal ends (Ac-X-NH₂). The key shows the tested identities of X (using a three-letter code) and the time length of the calculations, as well as the percentage modification to the force constants acting on the ω dihedral angles of N-methylated amino acids. **c)** Simulations of the open form at 490 K, using the 80% and 60% force field (FF) modifications to the force constants. The RMSD compared to the closed form is shown, along with the Mle-3 ω angle. The structure at the (ii) time-point (green) aligns well with the closed structure (orange), with a RMSD of 0.73 Å. **d)** Further simulations at different temperatures; i.e., 315, 393, and 448K. A simulation at 490 K with the 60% modification to the force constants applied only to the Mle-3 ω angle was also executed.

Figure 5. Molecular dynamics simulations of cyclosporin A in water. Starting with either the closed form (orange) or the open form (blue), simulations in an explicit water box were conducted at 315 and 490 K. **a)** In the upper panel, the root mean squared deviation (RMSD; backbone heavy atoms) of simulated structures compared to the closed structure for each simulation are shown as box plots. In the lower panel, the Mle-3 ω angle over the course of each simulation is shown in box plots. The angle corresponding to the ideal *cis* and *trans* bond orientations is shown for reference. The result for the simulation of the closed form in chloroform (CHCl₃) at 315 K is also shown for comparison. **b)** In the upper panel, the solvent-accessible surface area (SASA) for each simulation as box plots. In the lower panel, the polar surface area (PSA) distribution for the backbone polar groups of the simulated structures are shown.

Figure 6. *In silico* partitioning of cyclosporin A between water and chloroform. Simulations of cyclosporin A were conducted in a water–chloroform biphasic system at 490 K, and with the force constants modified to 60% of their original values (60% FF). **a)** The position of cyclosporin A relative to the membrane normal over the course of the simulation is shown. The root mean squared deviation (RMSD; backbone heavy atoms) of simulated structures compared to the closed structure is also plotted. An illustration of the simulation box is shown (top right). **b)** Box plots of the position of cyclosporin A along the chloroform normal for simulations in which cyclosporin A was not constrained, constrained in the closed conformation, and constrained in the open conformation. The grey shaded region corresponds to the chloroform phase of the simulation box.

Figure 7. NMR structural studies of cyclosporin A in membrane mimics. **a)** Chemical structures of chloroform and membrane mimics, including cyclohexane, SDS, and DPC. The chemical structure of POPC is also illustrated for comparison. The H_{α} chemical shifts of cyclosporin A in chloroform, cyclohexane, and DPC are shown. The chemical shifts of cyclosporin A in SDS were obtained from a previous report.²⁹ Below this plot is the H_{α} chemical shifts of cyclosporin A in cyclohexane, SDS and DPC, relative to those in chloroform (secondary shifts). **b)** 1D 1H spectra of cyclosporin A in cyclohexane and in the presence of DPC (and water). The temperature of the samples are shown, as well as the cyclosporin A to DPC ratio (w/w), where relevant. The peaks of the main conformation corresponding to the four backbone amides of cyclosporin A are labelled.

Figure 8. Membrane permeability of cyclosporin A *in silico*. Cyclosporin A was simulated in cyclohexane and in the presence of a POPC lipid bilayer with the 60% force constant modification (60% FF). **a)** The open structure was simulated in a box of explicit cyclohexane at 315, 393, 448, and 490 K. The root mean squared deviation (RMSD) of simulated structures compared to the closed structure is plotted. **b)** Position of cyclosporin A relative to the membrane normal and the root mean squared deviation (RMSD; backbone heavy atoms) of simulated structures (after equilibration) compared to the closed structure are plotted. To the

right is an illustration of the simulation box, showing that it is composed of a lipid bilayer. At the start of the simulation, cyclosporin A is placed above the lipid bilayer. **c)** Box plot of the RMSD dependence on exposure to water over the whole simulation. **d)** Simulations at 315, 393, and 490K. **e)** Area per lipid depending on the simulation temperature. **f)** Box plots of the position of cyclosporin A along the membrane normal for simulations (20–250 ns period of the production runs) in which cyclosporin A was not constrained, constrained in the closed conformation, and constrained in the open conformation. The grey shaded region corresponds to the lipid bilayer of the simulation box.

Figure 9. Membrane permeability of cyclosporin H and cyclic hexapeptides *in silico*. **a)** The sequence of cyclosporin H is shown at the top, with each residue represented using a three-letter code. The residue in bold at position 4 distinguishes cyclosporin H from cyclosporin A (i.e. Dmv instead of Mva). Below the sequence are ^1H 1D NMR spectra at 298K of cyclosporin H in various solvents, including a mixture of methanol and water (50% v/v methanol-d), acetonitrile and water (50% v/v acetonitrile-d₃), pure chloroform (chloroform-d), pure cyclohexane (cyclohexane-d₁₂), and in the presence of DPC micelles (at 1:100 and 1:250 peptide:DPC ratios). The solvent composition is shown above each spectrum. To the right is the backbone structure of cyclosporin H determined from crystals grown from methanol.⁴² **b)** The sequence of two cyclic hexapeptides referred to as cyclic peptide 1 and 13.¹⁶ (Cyclic peptide 1 was first reported as peptide 4²⁴). Cyclic peptide 13 differs from cyclic peptide 1 in that its first two amino acids (highlighted in bold) have methylated amides. To the right is the backbone structure of cyclic peptide 13 in 30% acetonitrile¹⁶ with the two N-methylated residues labeled. **c)** Position of cyclosporin H relative to the membrane normal with no constraints on the backbone and with the backbone constrained to the starting conformation;⁴² the position of the lipid bilayer is shaded grey. At the start of the simulation, cyclosporin H is placed above the lipid bilayer and simulated with the 60% force constant modification (60% FF). On the right are box plots of the position of cyclosporin H, and cyclic peptide 1 and 13, along the membrane normal for simulations in which the peptide was not constrained or constrained as indicated below the plots.

Figure 10. Role of conformational polymorphism in membrane permeability of cyclosporin

A. Outside of the membrane, cyclosporin A samples multiple different conformations, as indicated by the differently colored shapes. During permeation, it is likely that multiple states are sampled, with the proportion of each state changing depending on the phase (i.e. aqueous, membrane head group, membrane tail). In other words, it is likely that multiple permeation pathways exist, characterized by different combination of states at each phase. Each state has different physiochemical properties that affect its transition to the next phase; for example, the size of the solvation shell or the area of the open hydrophobic surface. Each state also interacts with the membrane differently, with some more able to negotiate through the polymeric net formed by the lipids.

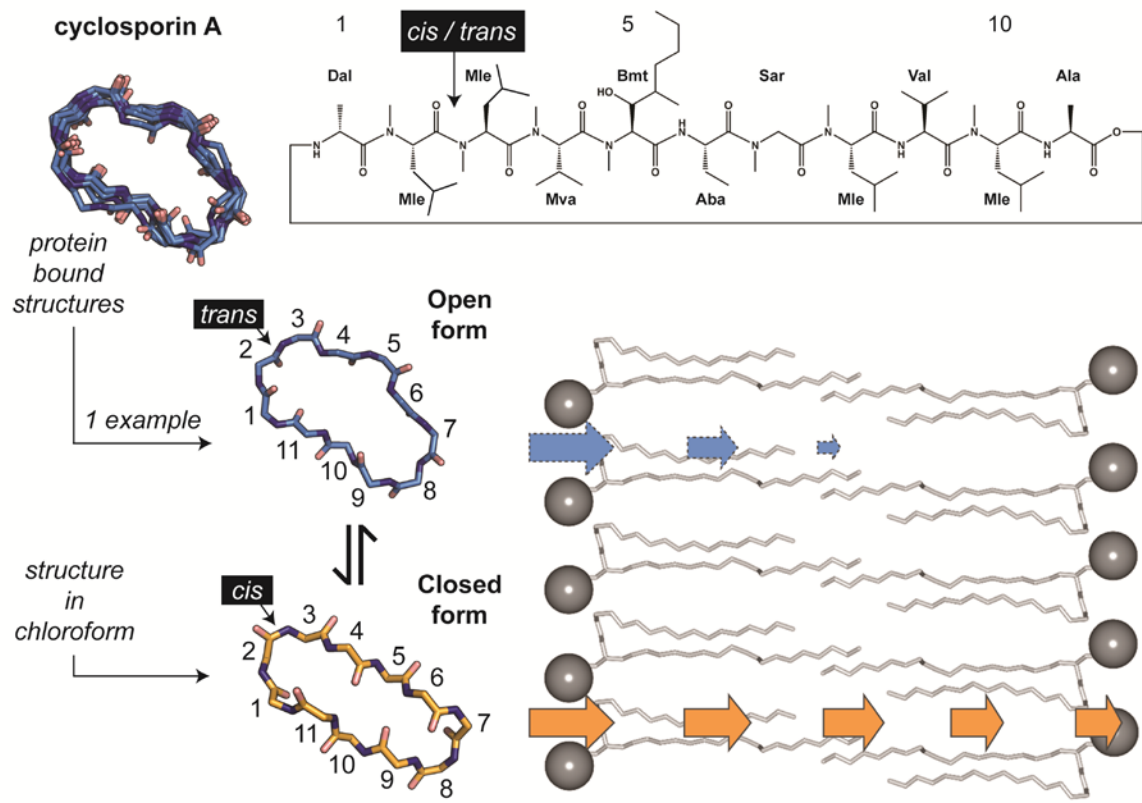


Figure 1

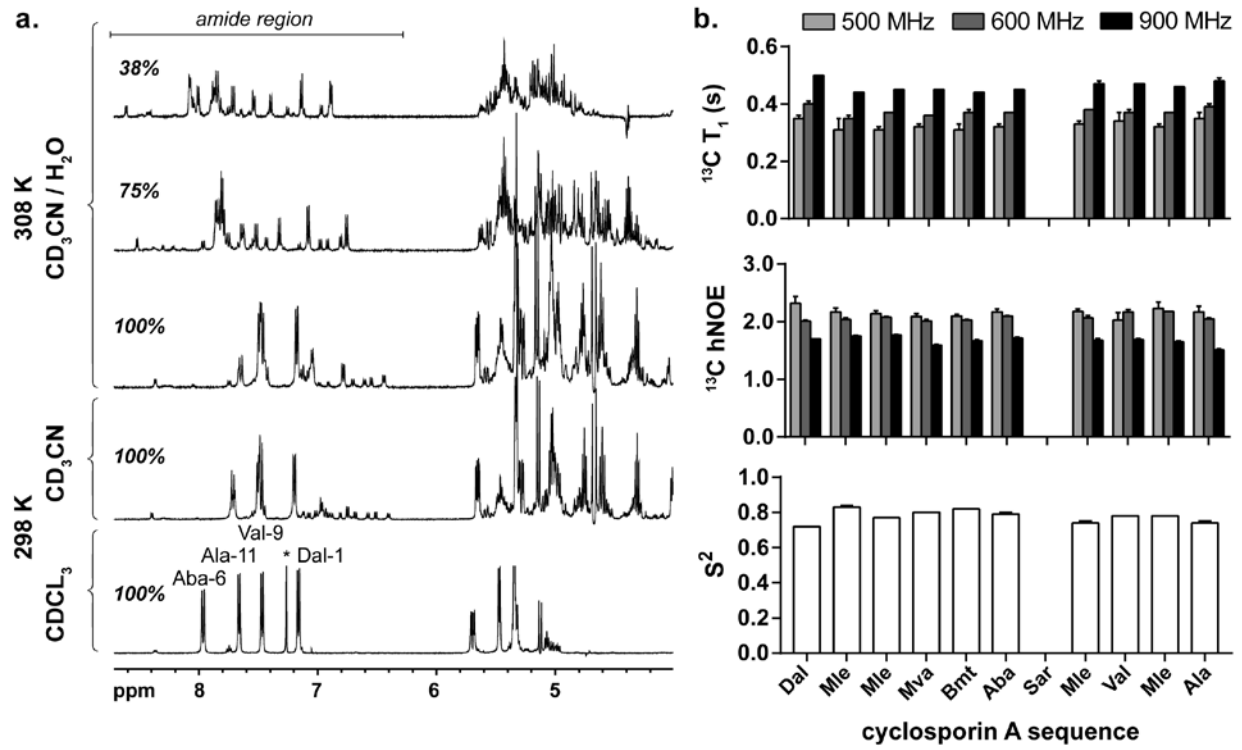


Figure 2

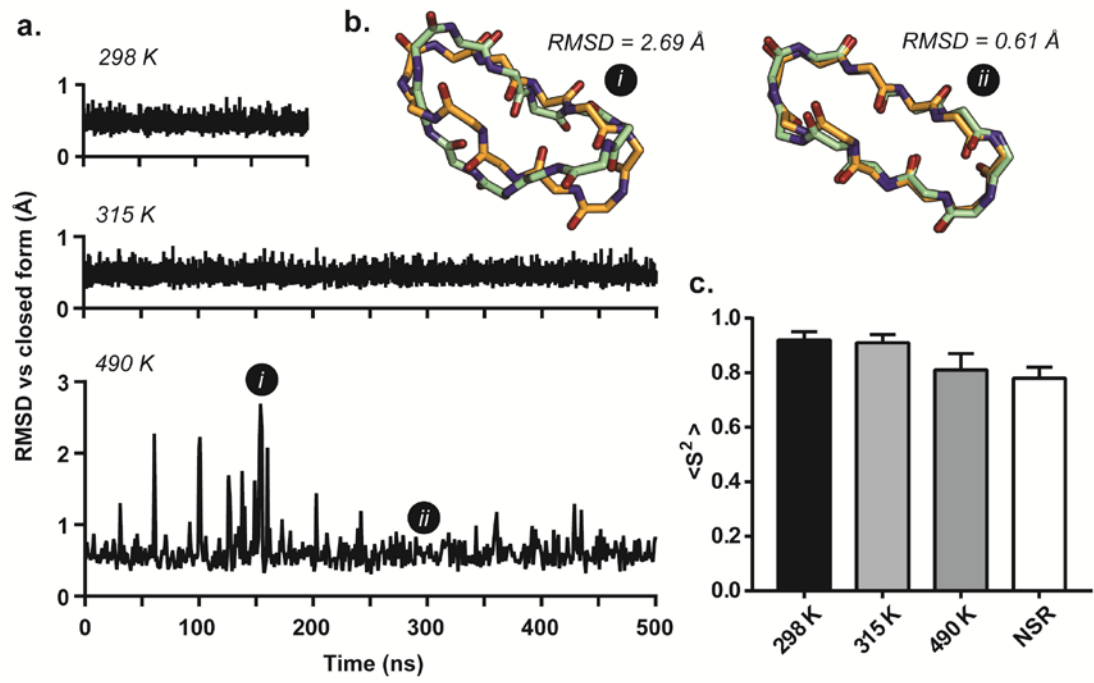


Figure 3

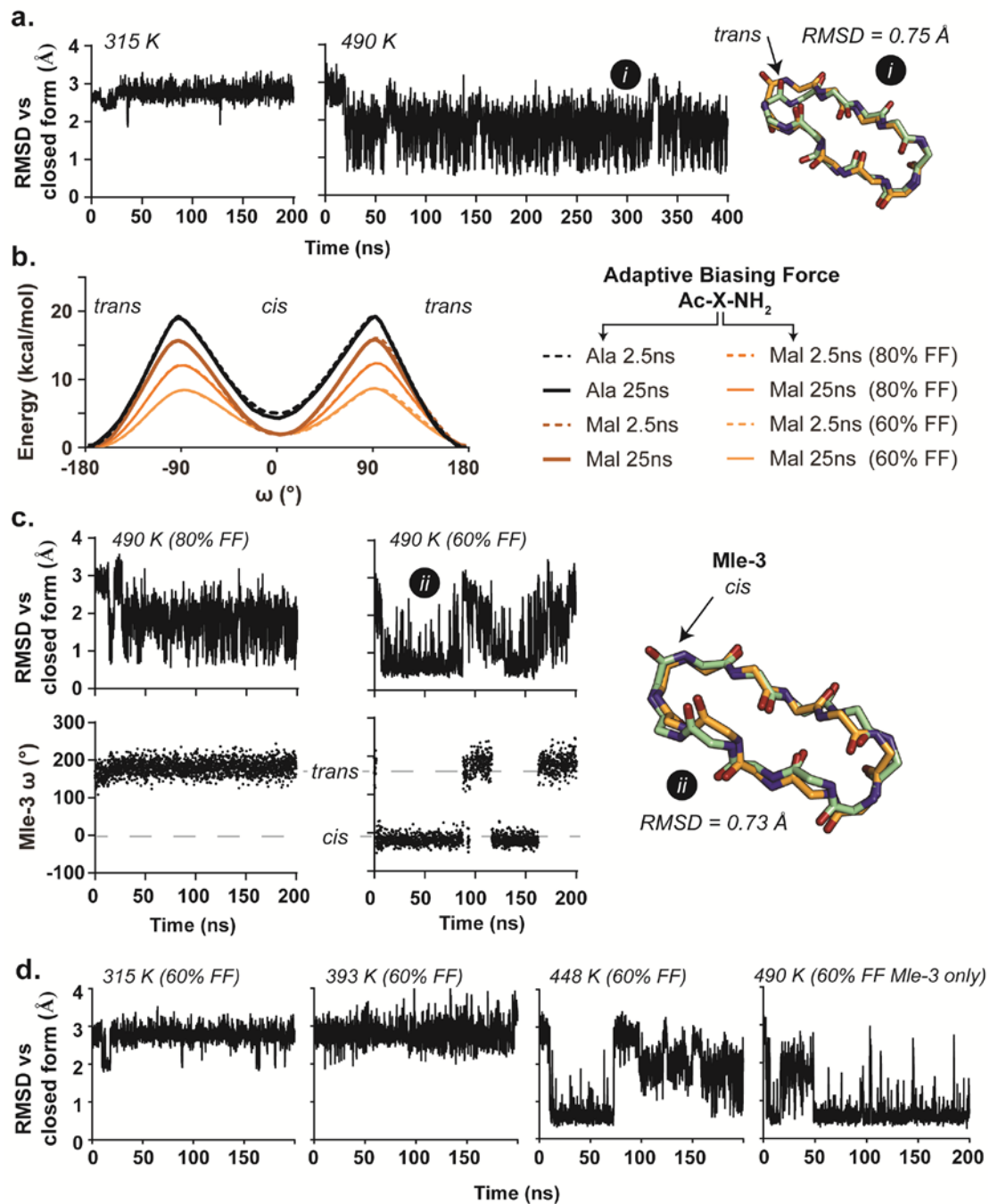


Figure 4

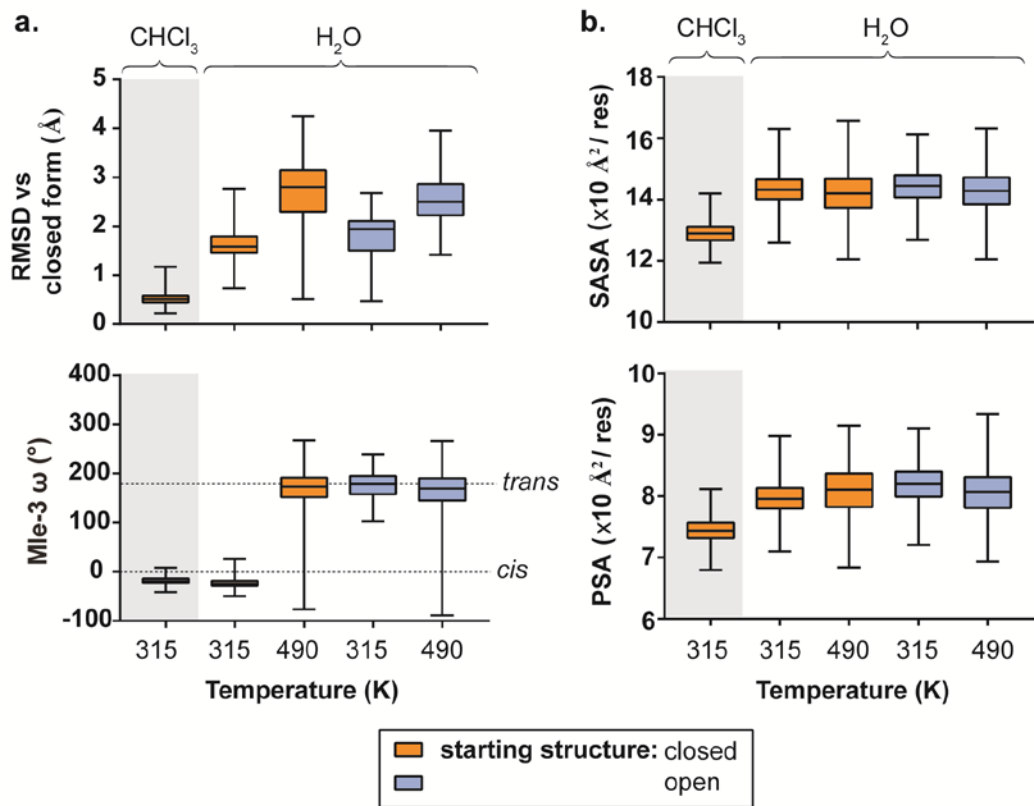


Figure 5

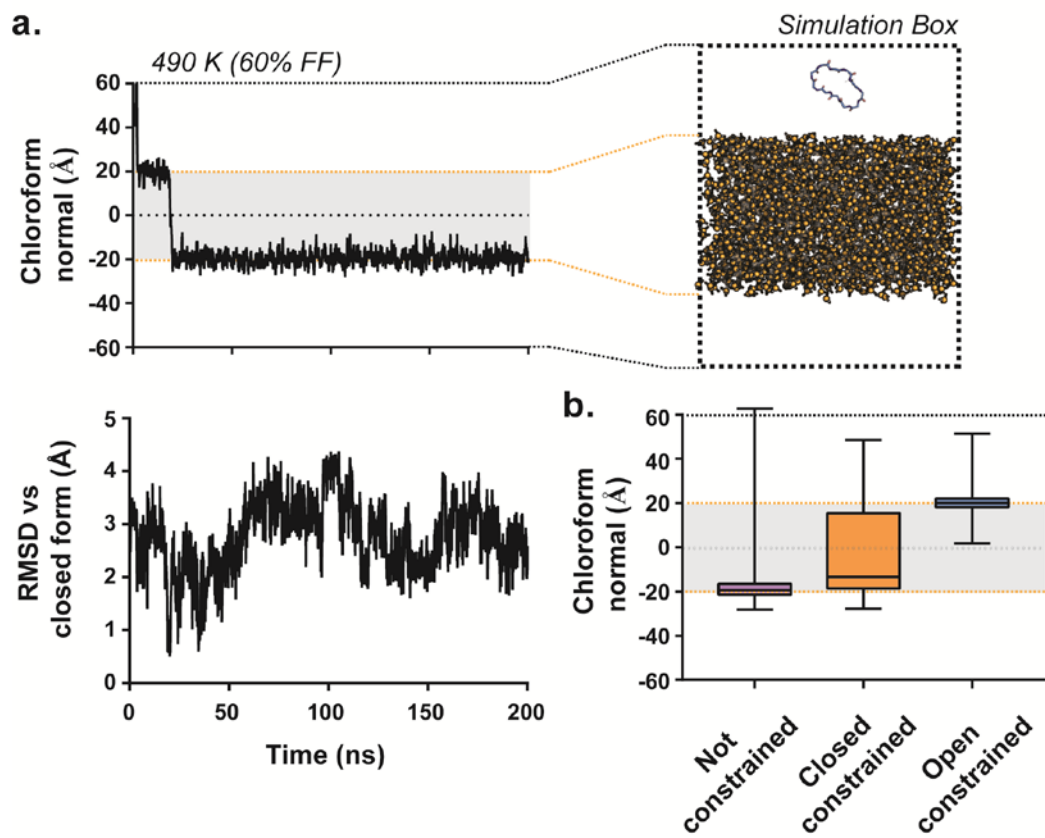


Figure 6

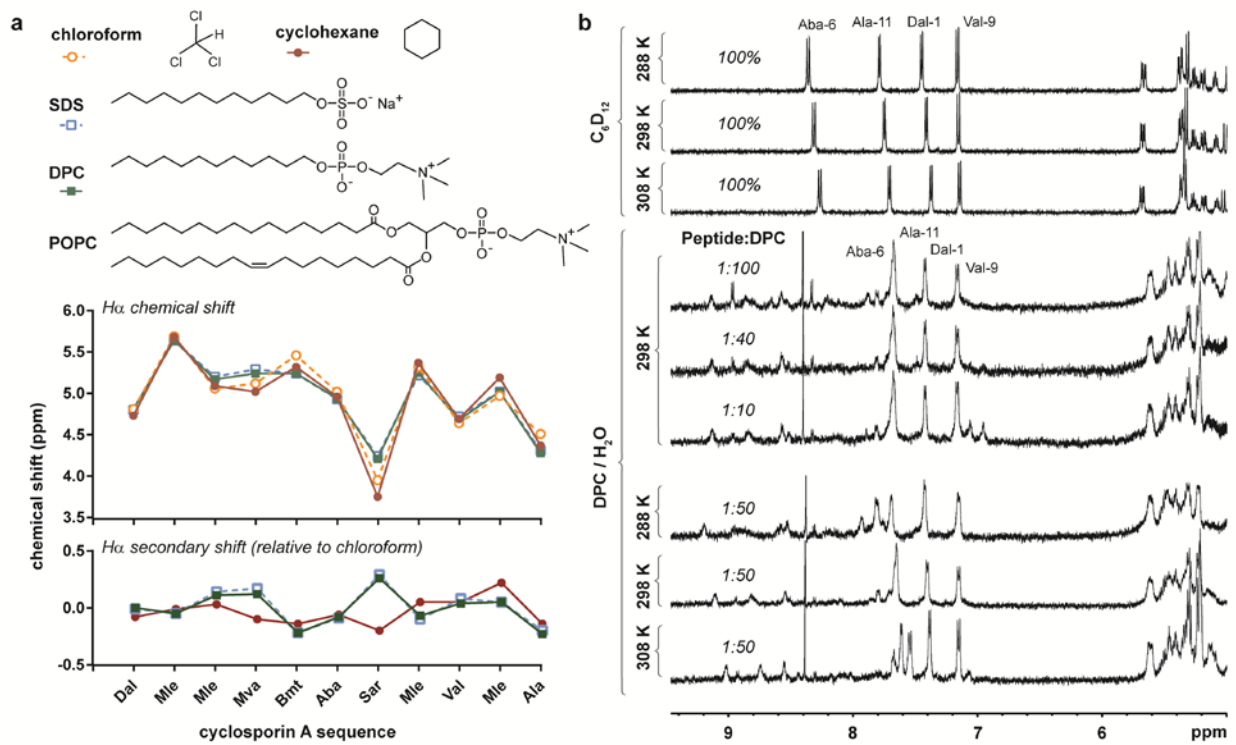


Figure 7

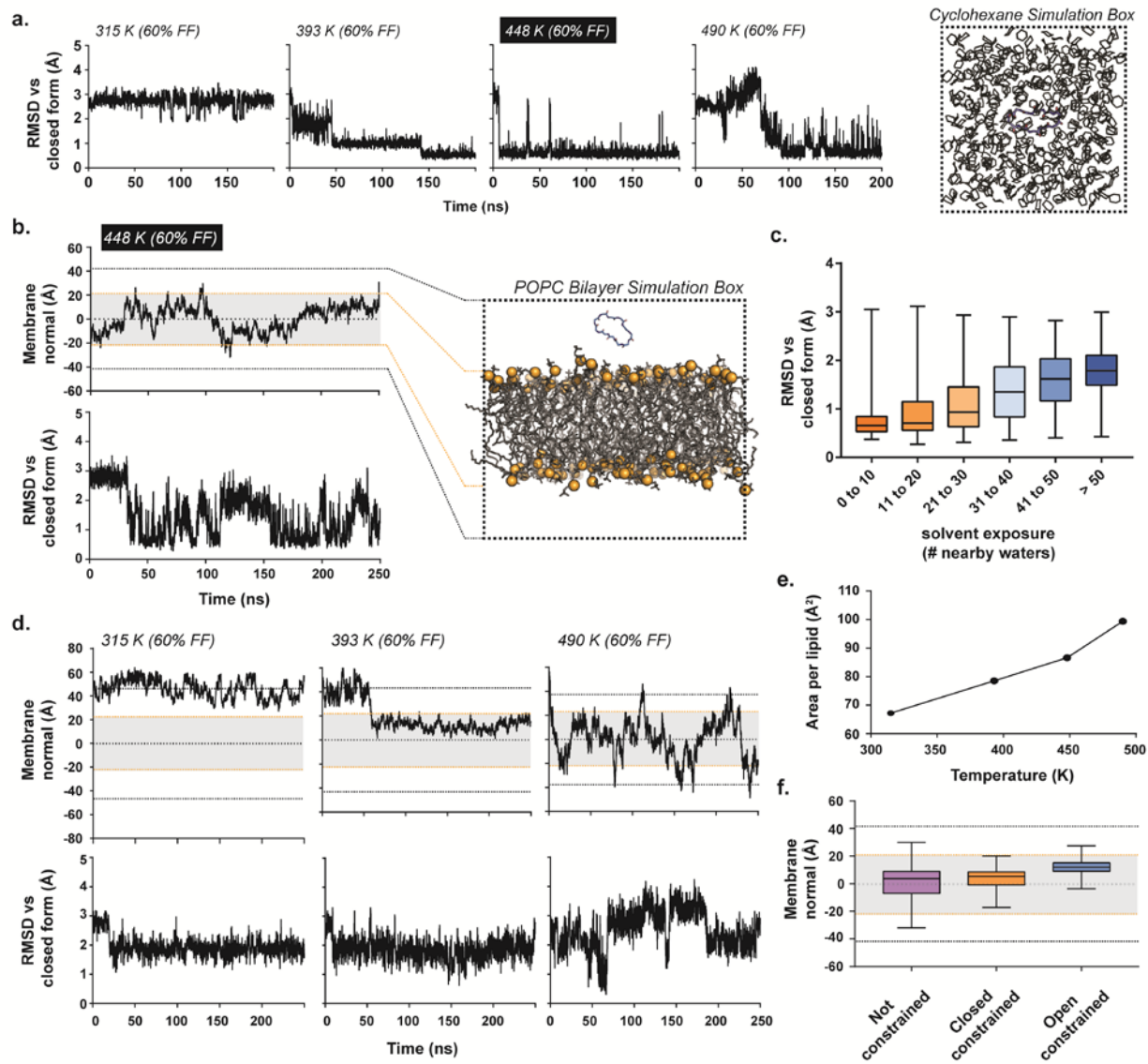


Figure 8

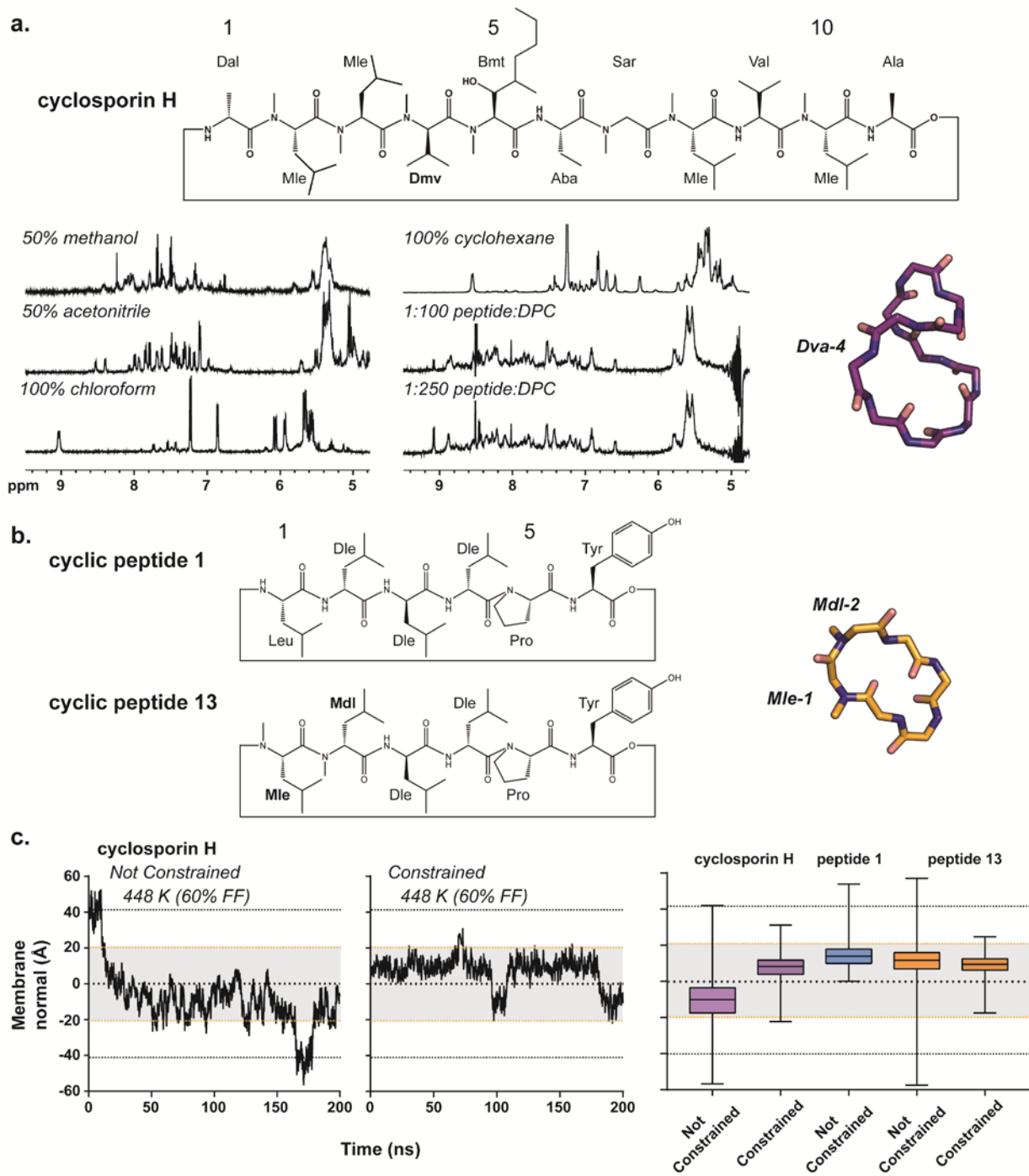


Figure 9

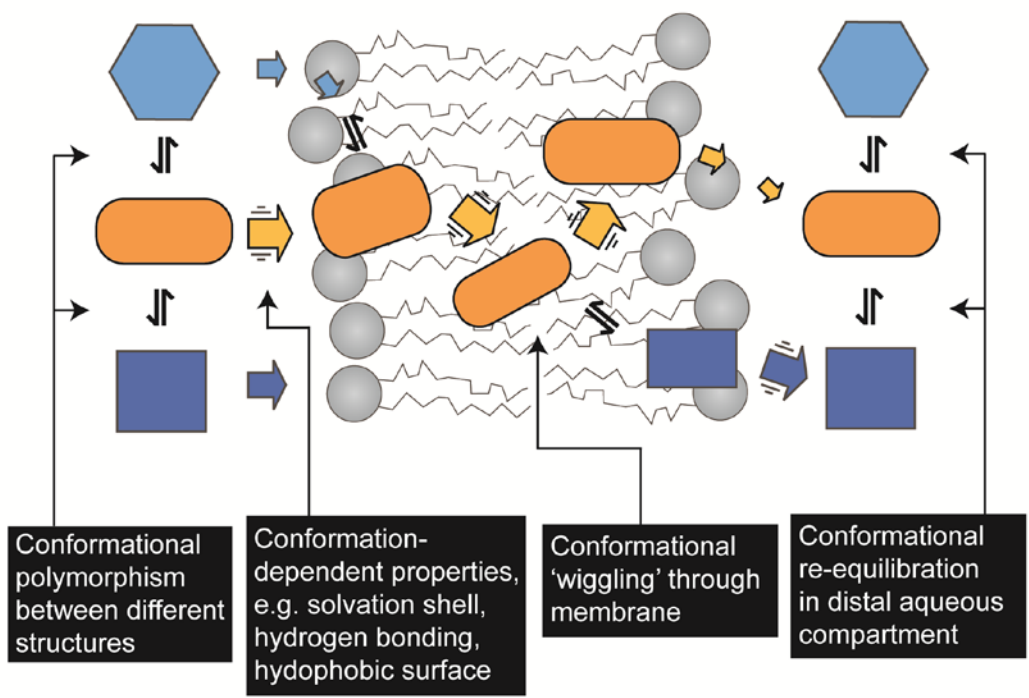
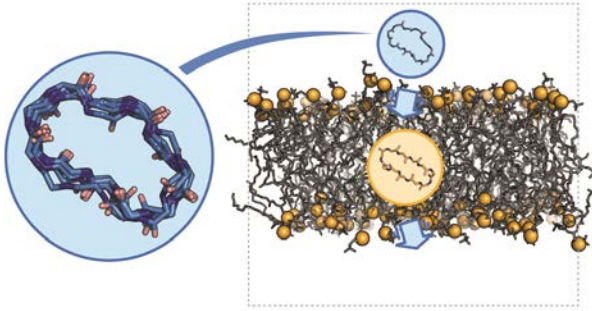


Figure 10



TOC Graphic